4314–4323 *Nucleic Acids Research, 1999, Vol. 27, No. 22*

Investigation of the recognition of an important uridine in an internal loop of a hairpin ribozyme prepared using post-synthetically modified oligonucleotides

Yasuo Komatsu*, Izumi Kumagai and Eiko Ohtsuka

Graduate School of Pharmaceutical Sciences, Hokkaido University, Sapporo 060-0812, Japan

Received as resubmission October 4, 1999; Accepted October 4, 1999

ABSTRACT

We introduced 4-thio- (^{4S}U), 2-thio- (^{2S}U), 4-*O*-methyluridine (^{4Me}U) and cytidine substitutions for U+2, which is an important base for cleavage in a substrate RNA. Oligonucleotides containing 4-thio- and 4-*O*-methyluridine were prepared by a new convenient post-synthetic modification method using a 4-*O*-*p*-nitrophenyl-uridine derivative. A hairpin ribozyme cleaved the substrate RNA with either C+2, ^{4S}U+2 or ^{4Me}U+2 at ~14-, 6- and 4-fold lower rates, respectively, than that of the natural substrate. In contrast, the substrate with a ^{2S}U+2 was cleaved with the same activity as the natural substrate. These results suggest that the O4 of U+2 is involved in hydrogen bonding at loop A, but the O2 of U+2 is not recognized by the active residues. Circular dichroism data of the ribozymes containing ^{4S}U+2 and ^{2S}U+2, as well as the susceptibility of the thiocarbonyl group to hydrogen peroxide, suggest that a conformational change of U+2 occurs during the domain docking in the cleavage reaction. We propose here the conformational change of U+2 from the ground state to the active molecule during the reaction.

INTRODUCTION

The hairpin ribozyme is the catalytic center in the self-cleaving domain of the negative strand of the satellite RNA of tobacco ringspot virus [sTobRV(–)], and it has both self-cleavage and ligation activities for RNA (1,2). The ribozyme consists of ~50 bases, and it can bind and cleave a substrate RNA at a specific site (3–6). The target sequence for the cleavage in the hairpin ribozyme is restricted to the 3′-side of the cleavage site, whereas the 5′-side sequence is important for cleavage by the hammerhead ribozyme. The target RNA is cleaved to yield a 2′,3′-cyclic phosphate and a 5′-hydroxyl group, and the cleavage is accelerated by the presence of magnesium ions, which also participate in a different way, in hammerhead ribozyme cleavage (7,8). The mechanism of the cleavage reaction has been investigated (9), and found to proceed by the in line mechanism, similar to the hammerhead ribozyme (5), although a phosphorothioate substitution in the cleavage site of a hairpin ribozyme does not affect the cleavage activity, in contrast to the hammerhead ribozyme (10,11). Recently, it has been shown that cobalt hexamine, which is an exchange-inert metal complex, can also induce cleavage activity, like the magnesium ions (12–14). These results indicate that the metal ion required for cleavage does not directly bind with the phosphate oxygens, but rather should function in outersphere binding with the ribozyme and as a structural factor for the active conformation of the ribozyme. It was also reported that hairpin ribozyme cleavage is catalyzed by aminoglycoside antibiotics (15).

The hairpin ribozyme consists of two stem–loop domains (domains I and II, shown in Fig. 1a), which involve internal loop A and loop B, respectively. Essential bases for the cleavage reaction in these loops have been identified by point mutations (16,17) and *in vitro* selection experiments (18,19). The global structure of the ribozyme has been studied by linker insertion experiments into the hinge region, which showed that the active structure for the hairpin ribozyme is a bent conformation (20,21). The requirement of a bent conformation for the cleavage reaction was proven by modification of the primary structure of the ribozyme (22,23). Recently, Lilley and co-workers have proven that the two domains are brought into close physical proximity by magnesium ions (24,25). Burke and co-workers reengineered the hairpin ribozyme and showed both active and inactive conformers (26). These conformers were also identified by kinetic analyses (27,28).

The secondary structure of loop B has been investigated by chemical modification (29) and UV crosslinking (30–32). Butcher and Burke proved the existence of a UV-photosensitive module in loop B from photo crosslinking, and proposed a secondary structure of loop B. Purine (33) functional groups and sugar requirements (33–35) were investigated by point mutation (16) and the insertion of modified nucleosides (33–35). These reuslts showed that most bases of the internal loop are essential, but U39 acts as a spacer nucleotide. Recently, NMR analysis of loop B has been reported (36) and showed that seven non-canonical base pairs are formed. Grasby and co-workers have investigated the active structure of loop B from cleavage reactions using modified pyrimidine nucleoside (37).

Cai and Tinoco studied the structure of domain I without domain II by an NMR method (38). The results showed that some of the bases in loop A form non-Watson–Crick base pairs, but U+2 following the cleavage site (Fig. 1a) does not contact any base and is splayed apart. Previous work indicated that a single base substitution of U+2 with A, G or C does not eliminate the cleavage activity completely but decreases it

*To whom correspondence should be addressed. Tel: +81 11 706 3976; Fax: +81 11 706 4989; Email: komatsu@pharm.hokudai.ac.jp

(39). Although an interesting structure was demonstrated from the NMR measurement of domain I alone, the structural change caused by the presence of domain II has not been probed.

We investigated the role of U+2 in loop A by substituting U+2 for 4-thio-, 2-thio- and 4-*O*-methyluridine, and measured the cleavage activities. Furthermore, photo crosslinking and circular dichroism (CD) measurement were carried out to study the location and the conformation of U+2 in the ribozyme. We describe the tertiary structure of loop A and speculate on the conformational changes of the ribozyme that occur during the reaction.

MATERIALS AND METHODS

General remarks

Thin-layer chromatography was done on Merck 60F254 coated plates. The silica gel and the neutralized silica gel used for column chromatography were Wakogel C-300 and ICN silica 60A, respectively. ^{1}H-NMR spectra were recorded with a JEOL EX-270 instrument using tetramethylsilane as an internal standard. ^{31}P-NMR were recorded with a JEOL GX-270 instrument with trimethyl phosphate. Chemical shifts are reported in parts per million (δ), and signals are expressed as s (singlet), d (doublet), t (triplet), q (quartet) and m (multiplet). All exchangeable protons were detected by the addition of D_2O.

5′-*O*-(4,4′-Dimethoxytrityl)-4-*O*-(4-nitrophenyl)uridine (2)

4-(4-Nitrophenoxy)-1-(β-D-ribofuranosyl) pyridine-2(1*H*)-one (**1**) (40) (914 mg, 2.5 mmol) which was coevaporated with pyridine, was dissolved in dry pyridine, after which dimethoxytrityl chloride (1.02 g, 3.0 mmol) was added. The reaction mixture was stirred for 1.5 h. Methanol was added to the aliquots to stop the reaction, and the solvent was evaporated under reduced pressure. The residue was dissolved in chloroform (40 ml) and was extracted with 0.5 M triethylammonium phosphate buffer (pH 7.0, 40 ml). The organic layer was filtered through 1PS filter paper (Whatman) and evaporated. After coevaporation with toluene, the residue was chromatographed by neutralized silica gel column chromatography (silica gel, 32.4 g) with 0–3% methanol in chloroform. The fractions containing compound **2** were combined, and after evaporation of the solvent, the colorless compound **2** (1.35 g, 2.20 mmol, 81%) was obtained.

^{1}H-NMR (270 MHz) [DMSO-d6] δ (p.p.m.): 8.37–8.32 (3H, m, H6, phenyl), 7.56–7.50 (2H, m, phenyl), 7.43–7.21 (9H, m, DMTr), 6.95–6.91 (4H, m, DMTr), 5.95 (1H, d, J = 7.9, H-5), 5.74 (1H, d, J = 2.0, H1′), 5.63 (1H, d, J = 4.62, 2′-OH), 5.13 (1H, t, J = 6.60, 3′-OH), 4.16 (1H, m, H2′), 4.07–4.02 (2H, m, H3′, H4′), 3.77 (6H, s, CH_3O-), 3.38 (2H, m, H5′). FAB-HRMS ($M+H^+$) 668.6787. Analysis calculated for $C_{36}H_{33}N_3O_{10}$: C, 64.79; H, 5.74; N, 6.29. Found: C, 64.34; H, 5.28; N, 5.87.

5′-*O*-(4,4′-Dimethoxytrityl)-2′-*O*-(*tert*-butyldimethylsilyl)-4-*O*-(4-nitrophenyl)uridine (3)

5′-*O*-(4,4′-Dimethoxytrityl)-4-*O*-(4-nitrophenyl)-uridine (**2**) (1.12g, 1.67 mmol), which was coevaporated with pyridine, was dissolved in dry tetrahydrofuran (16 ml). To the solution, dry pyridine (594 µl, 7.3 mmol) and silver nitrate (426 mg, 2.5 mmol) were added, and the reaction mixture was stirred at room temperature. After 15 min, *tert*-butyldimethylsilyl (TBDMS) chloride (429 mg, 2.8 mmol) was added, and the solution was stirred for 2.5 h. The reaction solution was filtered to remove the nitrate salt, and the solvent was evaporated. Triethylammonium phosphate buffer (0.5 M, pH 7.0, 20 ml) was added to the residue, and the solution was extracted with chloroform (20 ml). The aqueous layer was back extracted with chloroform (2 × 20 ml), and the combined organic layers were filtered through 1PS filter paper. The solvent was evaporated under reduced pressure, and was coevaporated with toluene to remove the pyridine. The residue was chromatographed on a neutralized silica gel column (silica gel 32.6 g) with 50–60% diethyl ether in hexane to give the 2′-*O*-silylated isomer (**3**)

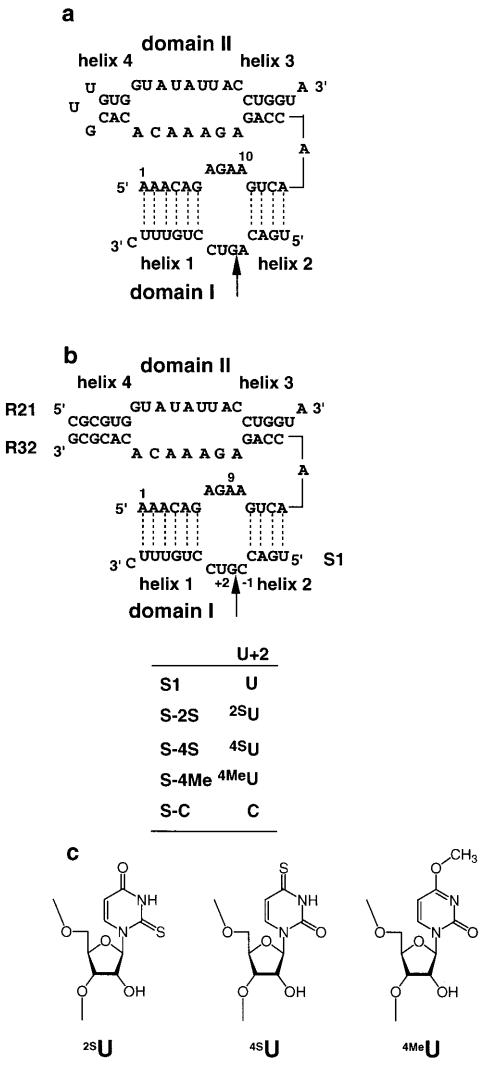

Figure 1. Secondary structures of hairpin ribozymes. (**a**) Wild type hairpin ribozyme, (**b**) complex of a two stranded hairpin ribozyme with a substrate. The substrate (S-4S, S-2S), with 4- or 2-thiouridine at U+2, was used for the cleavage reactions. S1 is the wild type substrate. (**c**) Structures of 4- and 2-thiouridines. Arrows indicate cleavage sites. Dotted lines indicate base pairs between the ribozyme and the substrate, and solid lines represent covalent bonds within the ribozyme.

(707 mg, 0.90 mmol, 54%) and the 3′-silylated isomer (305 mg, 0.39 mmol, 23%).

^{1}H-NMR (270 MHz) [DMSO-d6] δ (p.p.m.): 8.43(1H, d, J = 7.3, H6), 8.37(2H, m, H6, phenyl), 7.54 (2H, m, phenyl), 7.47–7.21 (9H, m, DMTr), 6.97–6.94 (4H, m, DMTr), 5.93 (1H, d, J = 7.3, H5), 5.72 (1H, s, H1′), 5.19 (1H, d, J = 5.9, 3′-OH), 4.30–4.20 (2H, m, H2′, H3′), 4.14–4.12 (1H, m, H4′), 3.79 (6H, s, CH_3O-), 3.52–3.40 (2H, m, H5′), 0.89 (9H, s, TBDMS tBu), 0.14 (3H, s, TBDMS CH_3-), 0.12 (3H, s, TBDMS CH_3-). FAB-HRMS (M+H$^+$) 782.9413. Analysis calculated for $C_{42}H_{47}N_3O_{10}Si$: C, 64.51; H, 6.06; N, 5.37. Found: C, 64.72; H, 6.13; N 5.16.

5′-*O*-(4,4′-Dimethoxytrityl)-3′-*O*-[(2-cyanoethoxy)(*N*,*N*-diisopropylamino)phosphino]-2′-*O*-(*tert*-butyldimethylsilyl)-4-*O*-(4-nitrophenyl)uridine (4)

5′-*O*-(4,4′-Dimethoxytrityl)-2′-*O*-(*tert*-butyldimethylsilyl)-4-*O*-(4-nitrophenyl)-uridine (**3**) (261 mg, 0.33 mmol) was coevaporated with pyridine and dissolved in dry tetrahydrofuran (1 ml). To the solution, 2,4,6-collidine (329 µl, 2.5 mmol), followed by *N*-methylimidazole (13.2 µl, 0.17 mmol), was added, and then (2-cyanoethoxy)(*N*,*N*-diisopropyl)chloro-phosphoramidite (95 µl, 0.43 mmol) was added dropwise to the solution, which was stirred. After 1 h, chloroform (20 ml) was added to the reaction solution and extraction was carried out using 0.5 M triethylammonium phosphate buffer (pH 7.0, 20 ml). The aqueous layer was back extracted with chloroform (20 ml). The combined organic layers were filtered through 1PS filter paper, and the solvent was evaporated under reduced pressure. After coevaporation with toluene, the residue was chromatographed on a neutralized silica gel column (silica gel, 7.5 g) with 0–3% ethylacetate in dichloromethane, and the compound (**4**) (195 mg, 0.20 mmol, 60%) was obtained.

^{1}H-NMR (270 MHz) [DMSO-d6] δ (p.p.m.): 8.67 (d, J = 7.3, H6, diastereomer), 8.62 (d, J = 7.3, H6, diastereomer), 8.27 (2H, d, J = 9.3, phenyl), 7.48–7.27 (11H, m, phenyl, DMTr), 6.90–6.86 (4H, m, DMTr), 5.82 (s, H-1′, diastereomer), 5.76 (s, H1′, diastereomer), 5.67 (d, J = 7.3, H5, diastereomer), 5.54 (d, J = 7.3, H5, diastereomer), 4.39–4.07 (3H, m, H2′, H3′, H4′), 3.82 (6H, s, CH_3O-), 3.74–3.51 (6H, m, cyanoethyl, H5′, diisopropylamino methines), 2.47–2.45 (2H, m, cyanoethyl), 1.56–1.11 (12H, m, diisopropylamino methyl), 0.91(9H, s, TBDMS tBu), 0.31, 0.27, 0.20, 0.15(6H, s, TBDMS CH_3-).

^{31}P-NMR (270 MHz) [$CDCl_3$](p.p.m.): 148.444, 146.022.

4-Thiouridine

4-(4-Nitrophenoxy)-1-(β-D-ribofuranosyl) pyridine-2(1*H*)-one (**2**) (184 mg, 0.5 mmol) was suspended in methanol (10 ml). Thioacetic acid (0.5 ml, 7.03 mmol) was added to the solution, and the reaction mixture was stirred at room temperature. After 30 min, the solvent was evaporated and the residue was chromatographed over a silica gel column (Wakogel C-300, 6.4 g) with 0–10% methanol in chloroform to give 4-thiouridine (143 mg, 0.54 mmol, 90%).

^{1}H-NMR (270 MHz) [DMSO-d6] δ (p.p.m.): 12.69 (1H, br, N-H), 7.84 (1H, d, J = 7.3, H5), 6.31 (2H, d, J = 7.9, H6), 5.73 (1H, d, J = 4.62, H1′), 5.44 (1H, d, J = 4.62, 2′-OH), 5.14–5.08 (2H, m, 2′-OH, 5′-OH), 4.06 (1H, m, H2′), 3.96 (1H, m, H3′), 3.87 (1H, m, H4′), 3.66 (1H, m, H5′a), 3.56 (1H, m, H5′b). FAB-HRMS (M+H+) 261.2721. Analysis calculated for $C_9H_{12}N_2O_5S$: C, 49.32; H, 4.22; N, 11.14. Found: C, 49.11; H, 4.22; N, 11.14.

Preparation of oligoribonucleotides

The 4-*O*-(*p*-nitrophenyl)-uridine (^{4nph}U) amidite unit was used with the DNA/RNA synthesizer and was assembled using standard RNA solid synthesis conditions, except for an extension of the coupling time (20 min). After the coupling reaction, the resin-bound oligoribonucleotides were treated with 10% thioacetic acid in methanol (1 ml) for 12 h at room temperature to convert ^{4nph}U to ^{4S}U. The resin was washed by CH_3CN. The oligoribonucleotides were cleaved from the resin and the protecting groups on the exocyclic amines and the phosphates were removed by treatment with 10% DBU (1,8-diazabicyclo-[5,4,0]-7-undecene) in methanol (1 ml) for 16 h at 30°C (41). The solution was filtered and concentrated to 1 ml. After 50% aqueous acetic acid (90 µl; 1.5 equivalent to DBU) was added, the solution was immediately passed through a Dowex50×8 (Na^+ form) ion exchange column, which was preequilibrated with methanol:H_2O (9:1) (42). The fractions containing the oligoribonucleotides were identified by UV absorbance (A_{260}) and combined. The 2′-*O*-TBDMS was removed by treatment with 50% triethylamine tris-hydrofluoride (Fluka) in dimethylsulfoxide (1 ml) for 24 h at room temperature. The completely deblocked oligoribonucleotides were desalted with Sephadex G25 (Pharmacia), and then purified by reverse phase and anion exchange column chromatographies, using µ-Bondasphere (C-18), 3.9 mm i.d. × 150 mm (Waters) and TSK gel DEAE-2SW, 4.6 mm i.d. × 250 mm (Tosoh), columns, respectively. The oligoribonucleotides containing ^{4S}U were traced by absorption at 334 nm and were detected by a photodiode array detector (Waters^{TM}996). The ^{4S}U-containing oligonucleotides (S-4S) were purified by reverse phase and anion exchange column chromatographies. µ-Bondasphere (C-18, 3.9 mm i.d. × 150 mm, Waters) was used as the reverse phase columun, and the gradient was 5–30% of B buffer content over 20 min [A buffer, 0.1 M TEAA (triethylamine acetate); B buffer, 25% acetonitrile, 0.1 M TEAA]. TSK gel DEAE-2SW (4.6 mm i.d. × 250 mm, Tosoh) was used as anion exchange column. The gradient was 25–45% B buffer content over 20 min (A buffer, 20% acetonitrile; B buffer, 20% acetonitrile, 2 M ammonium formate). The yield of S-4S substrate analog was 10%, and the conversion of ^{4nph}U to ^{4S}U was 94%.

Oligoribonucleotides containing a 4-*O*-methyluridine (^{4Me}U) were also prepared from the conversion of ^{4nph}U by a procedure similar to that used for ^{4S}U, except for the thioacetic acid treatment. ^{4nph}U in the resin-bound oligoribonucleotide was converted to ^{4Me}U during the deprotection of the exocyclic amino groups with 10% DBU in methanol (2 ml) at 30°C for 16 h. The desalting of DBU and deprotection of 2′-*O*-TBDMS group were carried out as described in the preparation of the oligonucleotide with a ^{4S}U. The ^{4Me}U-containing oligonucleotides (S-4Me) were purified by reverse phase and anion exchange column chromatographies. µ-Bondasphere (C-18, 3.9 mm i.d. × 150 mm, Waters) was used as the reverse phase columun, and the gradient was 5–25% B buffer content over 20 min (A buffer, 0.1 M TEAA; B buffer, 25% acetonitrile, 0.1 M TEAA). TSK gel DEAE-2SW (4.6 mm i.d. × 250 mm, Tosoh) was used as anion exchange column. The gradient was 20–40% B buffer content over 20 min (A buffer, 20% acetonitrile; B buffer, 20% acetonitrile, 2 M ammonium formate). The yield of S-4Me was 10%, and that of the conversion step from ^{4nph}U to ^{4Me}U was 96%.

The coupling time of the ^{2S}U amidite unit was 20 min, and the oxidation step was carried out for 12 min with 1.0 M *tert*-butylhydroperoxide, which was prepared from the dilution of 7.9 M *tert*-butylhydroperoxide in a di-*tert*-butylhydroperoxide solution with acetonitrile (43). Deprotection of the exocyclic amino and 2′-*O*-TBDMS groups were carried out by the same method as S-4S preparation. The ^{2S}U containing oligonucleotides (S-2S) were purified by reverse phase and anion exchange column chromatographies, using μ-Bondasphere (C-18), 3.9 mm i.d. × 150 mm (Waters) and TSK gel DEAE-2SW (4.6 mm i.d. × 250 mm, Tosoh), columns, respectively. The gradient conditions used for these chromatographies were the same as that for S-4Me purification. The yield of S-2S was 27%.

The purity and nucleotide composition of the substrate containing ^{4S}U, ^{2S}U and ^{4Me}U were identified by complete digestion with snake venom phosphodiesterase and alkaline phosphatase, followed by analyses by reverse phase HPLC using standard compounds as previously reported (44). The composition analysis of ^{2S}U and ^{4Me}U were carried out using a reverse phase (C-18) column (Inertsil ODS-3, 4.6 mm i.d. × 250 mm, GL Sci. Inc.). Gradient was 0–30% B buffer content over 30 min (A buffer, 0.1 M TEAA; B buffer, 50% acetonitrile, 0.1 M TEAA). However, the analysis of ^{4S}U was not separable by Inertsil ODS-3 column, and μ-Bondasphere (C-18, 3.9 mm i.d. × 150 mm, Waters) was used with a gradient of 0–25% B buffer content over 20 min (A buffer, 0.1 M TEAA; B buffer, 50% acetonitrile, 0.1 M TEAA).

Cleavage reaction

Single turnover reaction. The 5′-ends of the substrates (S1, S-4S, S-2S, S-4Me and S-C) were labeled with ^{32}P for the cleavage reactions. These 5′-end-labeled substrates and the ribozyme (E32-E21) were dissolved separately in cleavage buffer (40 mM Tris–HCl pH 7.5, 12 mM $MgCl_2$, 2 mM spermidine–3HCl) to concentrations of 40 nM and 4 μM, respectively. The substrate in the cleavage buffer (6 μl) was heated at 65°C for 2 min and immediately transferred to an ice-bath, and an equal volume of ribozyme solution, which had been denatured at 65°C for 2 min and annealed in an ice-bath for 10 min, was added to the denatured substrate to start the reaction. The final concentrations of substrate (S1, S-4S, S-2S, S-4Me or S-C) and ribozyme were 10 nM and 1 μM, respectively, and the total volume was 12 μl. The reaction mixture was incubated at 37°C, and aliquots were taken at time intervals and added to loading solution (10 M urea, 50 mM Na_2EDTA) to stop the reaction. The aliquots were fractionated by electrophoresis on a 20% polyacrylamide gel (acrylamide:bisacrylamide, 19:1) containing 8 M urea. The gel was dried and exposed to an imaging plate for bioimaging analysis (Fujix BAS2000). The observed rate constants were calculated from a least squares fit of the data points on a plot of the percentages of cleavage versus time, using the following equation $P/P + S = A[1 - \exp(-kobs \times t)]$, where P is the concentration of the cleavage products, S is the concentration of the remaining substrate, and A is a factor showing the cleavable substrate ([cleavable substrate] = A[total substrate]).

Multiple turnover reaction. The ribozyme strands (E32 and E21) and the substrate were dissolved separately in the cleavage buffer. The ribozyme was denatured by heating at 65°C for 2 min, followed by cooling in an ice-bath for 10 min. An equal volume of the ribozyme solution was added to the substrate solution, which was previously denatured at 65°C for 2 min and then cooled in an ice bath. The reaction was started in a final volume of 12 μl, containing 16 nM ribozyme strands and 20–300 nM substrate, and was incubated at 37°C. Cleavage products were analyzed as described above for the single turnover reaction. From the cleavage products, the initial velocities were calculated over a specific time range (<10% cleavage), and the kinetic parameters were obtained from Hanes–Woolf plots.

Cleavage reactions at various magnesium ion concentrations

The ribozyme strands (E32 and E21) and the substrate (S1, S-4S, S-2S, S-4Me or S-C) were dissolved in annealing buffer (80 mM Tris–HCl pH 7.5, 4 mM spermidine–3HCl) without magnesium ions, to concentrations of 4 μM and 40 nM, respectively. An equal volume of magnesium chloride solution (4–200 mM, 7 μl) was added to the solution of the ribozyme–substrate complex. The reaction was started in a final volume of 14 μl, containing 2 μM ribozyme and 20 nM substrate, and was incubated at 37°C. The cleavage products were analyzed as described for the single turnover reaction. From the cleavage products, the initial velocities (V) were calculated. The association constants ($K_{[Mg^{2+}]}$) of the magnesium ions were determined from a least squares fit of the data points on a plot of the initial velocities of cleavage versus the concentrations of magnesium ions, using the following equation:

$$V = (V_{max} \times [Mg^{2+}])/(K_{[Mg^{2+}]} + [Mg^{2+}])$$ (45).

Photo crosslinking

S-4S (Fig. 1b) in the cleavage buffer was heated at 65°C for 2 min, and then cooled in an ice bath. An equal volume of the substrate solution was added to the ribozyme solution, which was also dissolved in the cleavage buffer. The combined solution (14 μl), containing both the substrate (750 nM) and the ribozyme (1.5 μM), was exposed to UV irradiation (365 nm) for 30 min, either on ice or at room temperature. After the reaction solution was mixed with the loading solution, the products were fractionated by electrophoresis on a 20% polyacrylamide gel containing 8 M urea. The bands of the crosslinked products were excised from the gel, and the crosslinked products were eluted from the gel slice in distilled water. The eluted products were purified on a NENSORB^{TM}20 column (Du Pont).

After the purification of the crosslinked products, the crosslinked sites were determined by limited alkaline hydrolysis and by base specific RNases.

CD measurements

Hairpin ribozyme components [domains I and (I+II)], dissolved in the cleavage buffer (300 μl) to a concentration of 20 μM, were heated at 90°C for 2 min, and then immediately transferred to an ice bath. After 1 h on the ice bath, the CD spectra were measured using a 1 mm path length cell. Otherwise, the temperature was not specified.

H_2O_2 treatment. Domain I or domain (I+II), dissolved in the cleavage buffer (20 μM; 300 μl), was heated at 90°C for 2 min, and then immediately transferred to an ice bath. After 1 h on the ice bath, 1 and 30% H_2O_2 aqueous solutions (1 μl) were added for the reaction of the ribozymes containing 4-thio and 2-thiouridine, respectively. Since H_2O_2 converts 4-thiouridine

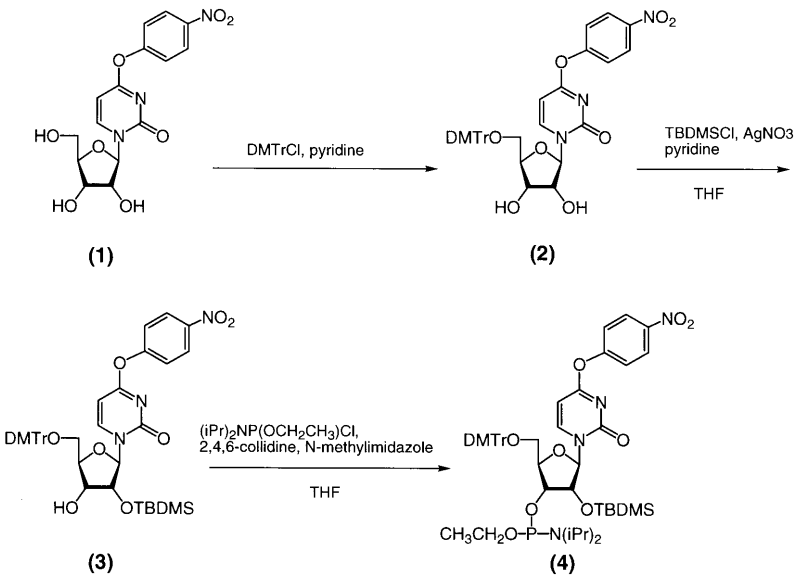

Scheme 1.

to uridine, the CD spectra of both complexes containing a uridine at +2 were used to monitor the complete reaction of H_2O_2. Percentages of the remaining thiocarbonyl group ($[\theta]_s$) were obtained by $[\theta]_s = 100[1 - ([\theta]_t - [\theta]0)/([\theta]_\infty - \theta]0)]$. Each $[\theta]$ was the peak intensity at 335 nm. Half-lives were determined by plots of $[\theta]_s$ versus various times. $[\theta]_t$, $[\theta]$ value after t min; $[\theta]_0$, $[\theta]$ before the reaction with H_2O_2; $[\theta]_\infty$, $[\theta]$ of the complex containing a uridine at position +2.

RESULTS AND DISCUSSION

Post-synthetic modification of oligonucleotides using 4-*O*-*p*-nitrophenyluridine

Oligoribonucleotides containing 4-thiouridine can be prepared by using S-cyanoethyl-protected 4-thiouridine as a coupling unit, followed by deprotection (46,47). However, S-cyanoethyl-protected 4-thiouridine cannot be converted to any other nucleoside analog. Although a post-synthetic modification for the synthesis of 4-thiouridine-containing oligonucleotides using 4-*O*-triazolouridine was reported (41), it is too unstable for a large-scale preparation. Thus, we planned to use 4-*O*-*p*-nitrophenyl-uridine for the modification of oligonucleotide analogs. As shown in Scheme 1, 4-*O*-*p*-nitrophenyl-uridine (^{4nph}U) (**1**) (40) was prepared from uridine, and the primary hydroxyl group was protected by dimethoxytrityl chloride to give compound **2**. The 2′-hydroxyl group was silylated with TBDMS chloride in the presence of silver nitrate and pyridine (48) since the *p*-nitrophenol group is unstable in either dimethylamino pyridine or imidazole. The 2′-*O*-TBDMS isomer (**3**) was separated from the 3′-isomer. The 3′-hydroxyl group of compound **3** was phosphorylated by a standard method (49) in the presence of collidine and *N*-methylimidazole, which did not cleave the *p*-nitrophenol group.

To prepare the substrate analogs (S-4S and S-4Me shown in Fig. 1b) with 4-thio- and 4-*O*-methyluridne, respectively, at position +2 in S1, the ^{4nph}U amidite unit was assembled by a standard method. After the synthesis, the resin-bound oligo-ribonucleotide was treated with thioacetic acid to convert ^{4nph}U to ^{4S}U, by the procedure used for the conversion of 4-*O*-triazolouridine (41). The ^{4nph}U in the resin-bound oligonucleotide was also converted to 4-*O*-methyluridine (^{4Me}U), by treatment with DBU/methanol during the deprotection of the exocyclic amines and the cleavage from the support. The DBU was removed by the ion exchange resin, and the oligoribonucleotide was purified by reverse phase and anion exchange column chromatography. The presence of ^{4S}U or ^{4Me}U was analyzed by complete enzymatic digestions of S-4S and S-4Me. The S-4S substrate analog was further characterized by polyacrylamide gel electrophoresis with a mercury derivative (50).

2-Thiouridine was prepared from the glycosylation of 2-thiouracil and D-ribose, as previously described (43). The S-2S substrate, with ^{2S}U at position +2, was synthesized by the phosphoramidite method (Fig. 1b).

Cleavage reaction of RNA containing ^{4S}U, ^{4Me}U, C or ^{2S}U

Besides three substrate analogs (S-4S, S-2S and S-4Me), S-C which has a cytidine base at position +2, was prepared to compare the cleavage activity. The 5′-ends of S-4S, S-2S, S-4Me, S-C and S1 were labeled with ^{32}P. Since it has been reported that the sulfur atom of ^{4S}U decomposes by irradiation with the ^{32}P-derived β-emission (50), the stability of S-4S was checked by fractionation on a polyacylamide gel in which a mercury derivative was covalently immobilized. Although a slight amount of ^{4S}U desulfurization was detected after ^{32}P labeling, depending on the amount of time after labeling, it was immediately used for the cleavage reactions. The three substrate analogs (S-4S, S-2S and S-4Me) and the natural substrate (S1) were subjected to cleavage by the two stranded ribozymes (R32-R21) (51) shown in Figure 1b. Cleavage reactions were carried out under single turnover conditions. S-2S was cleaved with almost the same activity as that of the natural substrate, whereas the cleavage rate constants for S-4S and S-4Me were ~6- and 4-fold lower than that of S1, respectively (Table 1). Under multiple turnover conditions, S-2S indicated slightly higher

Table 1. Kinetic parameters of cleavage reactions with natural and modified substrates

Substrate	k_{obs} (min^{-1})	K_m (nM)	k_{cat} (min^{-1})	k_{cat}/K_m ($min^{-1}\cdot nM^{-1}$)	$K_{Mg^{2+}}$ (mM)
S1	0.34 ± 0.01	26 ± 0.55	0.15 ± 0.04	5.8×10^{-3}	3.8 ± 0.3
S-2S	0.24 ± 0.009	139 ± 10	0.49 ± 0.06	3.5×10^{-3}	8.8 ± 1.5
S-4S	0.059 ± 0.002	44 ± 4	0.0089 ± 0.0014	2.0×10^{-4}	4.7 ± 0.7
S-4Me	0.093 ± 0.004	29 ± 12	0.082 ± 0.003	2.8×10^{-3}	0.9 ± 0.1
S-C	0.025 ± 0.0003	26 ± 9	0.029 ± 0.005	1.1×10^{-3}	13.4 ± 2.0

k_{cat}/K_m value than that of the wild-type substrate, although the K_m of S-2S was larger than that of S1. The k_{cat} for S-4S was 20-fold lower than that of the natural substrate. The k_{cat} values for S-4Me, and S-C were 2- and 5-fold lower than that of the natural substrates, respectively. On the other hand, S-2S indicated about a 3-fold higher k_{cat} than that of the control substrate. The k_{cat}/K_m value for S-4S was ~30-fold lower than that of the natural substrate. These results suggest that the O4 of U+2 is more important for the cleavage activity than the O2 of U+2. The large K_m of S-2S, suggests that the O2 of U+2 might be involved in binding with the ribozyme; however, the O2 does not influence the chemical step.

The exocyclic oxygens of a uridine can become hydrogen acceptors; however, sulfur substitution of the oxygen is supposed to decrease the stability of the hydrogen bond. Since the structure of the N3 of uridine is the same between ^{4S}U and ^{2S}U, the difference in the cleavage activity between S-4S and S-2S indicates that the O4 of U+2 is more important than the O2 of U+2 for the cleavage reactions. The O4 may be involved in the hydrogen bond, whereas the O2 of U+2 may not participate in the active loop structure. S-4Me was cleaved slightly more efficiently than S-4S. The substrate with a ^{4Me}U also was cleaved ~4-fold faster than S-C with a cytidine at position +2, under single turnover conditions. From the crystal structure of 4-*O*-methyluridine, the methyl group of ^{4Me}U assumes the *syn*-periplanar conformation, as shown in Figure 1c (52,53). Therefore, the O4 of ^{4Me}U could be a weak hydrogen bond acceptor, and then S-4Me might be cleaved more efficiently than S-C. The 4-amino group of C+2 is a hydrogen donor, and S-C was cleaved at a 14-fold lower rate than the natural substrate under single turnover conditions. S-4S had slightly higher cleavage activity than S-C. The reason for this might be that the sulfur atom of S-4S might serve as a weak hydrogen acceptor.

To investigate whether the O4 of U+2 participates in magnesium ion binding, the cleavage reactions were carried out at various magnesium ion concentrations, and the initial velocities were measured (Fig. 2). The association constants and V_{max} were calculated as reported (45). The cleavage activities of S-4S, S-4Me and S-C could not reach that of S1, even at high magnesium ion concentrations (Table 1). On the other hand, S-2S was cleaved as efficiently as the natural substrate at all magnesium ion concentrations. High concentrations of magnesium ions could not compensate for the cleavage activities of S-4S, S-4Me and S-C. The V_{max}s of S-4S, S-4Me and S-C were 6-, 4- and 8-fold lower than that of S1, respectively. The difference in the activities might be derived from the structural distortion induced by the O4 modification. The association constants for the magnesium

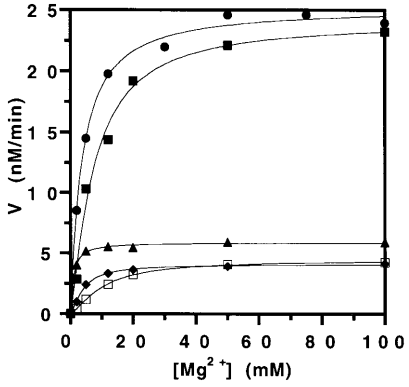

Figure 2. Plot of initial velocities versus concentrations of magnesium ions. S1 (circles), S-2S (solid squares), S-4Me (triangles), S-4S (diamonds) and S-C (open squares) were subjected to cleavage reactions by the ribozyme (R32-R21) with various concentrations of magnesium ions.

ion of S-4S indicated almost the same activity as the control substrate. This result suggests that the O4 of U+2 is not involved with magnesium ion binding, but with the formation of hydrogen bonds. The reason for the low value of the association constant of S-4Me is not clear; however, steric hindrance of the methyl group of ^{4Me}U might deform the internal loop structure.

Tinoco and co-workers revealed that U+2 is splayed apart in the stem–loop structure of domain I, in the absence of domain II, by NMR analysis (38). In the loop A structure, the O4′ of the sugar of U+2 forms hydrogen bonds with either the imino or amino proton of G8, and there was no evidence for any interaction with the base of U+2. The present result that the O4 of U+2 is involved with the cleavage step, in contrast to the O2 of U+2, cannot be elucidated by the NMR structure. Therefore, the conformational change of U+2 was considered to occur when domain I interacts with domain II. The O4 of U+2 does not contact other residues in domain I itself, but may become a hydrogen acceptor in the active bent structure. The NMR data also suggest that U+2 adopts the flexible conformation in domain I, because of the millisecond conformational change of U+2. Therefore, U+2 could easily adopt the conformational change by domain docking.

The NMR structure of U+2 indicates the ground state conformation, and this structure of U+2 may change from a bulged structure to a paired form in a transition state. Recently, Burke and co-workers also suggested that a conformational

change occurs in the ribozyme after the initial domain docking in the hairpin ribozyme, based on the results of a fluorescence resonance energy transfer experiment (54).

Photo crosslinking reactions using S-4S

Although S-4S was cleaved at a 6-fold lower rate than that of the natural substrate, S-4S could be cleaved faster than S-C. Therefore, photo crosslinking experiments with S-4S were carried out to investigate the tertiary structure of loop A. To prevent cleavage of the substrate during the photo reaction, photo crosslinking was carried out using S-4S(me), which has 2′-*O*-methylcytidine at the cleavage site (C-1). S-4S(me) was combined with R14 and R32-R21 to form domains I and (I+II), respectively (Fig. 3a). The S-4S(me)–R32 complex [domain (I+II′)] was also used as an inactive molecule. The 5′-end of either R14, R32 or R21 was labeled with ^{32}P for photo crosslinking. Crosslinked products, CL(I) (lane 3), CL(I+II′) (lane 4), and CL(I+II) (lane 5), were generated from UV irradiation of domains I, (I+II′) and (I+II), respectively (Fig. 3b). S-4S(me) did not crosslink with R21 in domain (I+II), but with R14 and R32 in the three complexes. The CL(I), CL(I+II′) and CL(I+II) complexes were recovered from the gel, and the crosslinking sites of these products were determined by limited alkaline hydrolysis (Fig. 4a) (28). For CL(I), the crosslinked residue in R14 was A9 (Fig. 4a, lane 3). The crosslinked sites for CL(I+II′) and CL(I+II) were also A9 in R32 (Fig. 4a, lanes 7 and 12). The crosslinked sites in the S-4S(me) strand of these crosslinked products were identified as ^{4S}U+2, as expected (data not shown). These results indicate that ^{4S}U+2 in S-4S(me) of the three complexes crosslinked with A9 in the complementary strand, as shown in Figure 4b. The percentages of crosslinked products were measured at various times, and the yields of the crosslinked products were not changed after 30 min of UV irradiation. The yields of CL(I), CL(I+II′) and CL(I+II) were ~50% after 30 min of irradiation. Although the yields of the crosslinking reactions were also measured at various concentrations of magnesium ions, the three complexes had almost the same crosslinking yields.

Previous hairpin ribozyme crosslinking experiments had been carried out using an all deoxy substrate, which contained a 2′-deoxy-4-thiothymidine substituted for U+2 (32). The 2′-deoxy-4-thiothymidine substituted for U+2 was crosslinked with A7 and A5, in addition to A9 in the complementary strand. On the other hand, S-4S(me) only contained ribonucleotides and crosslinked only with A9. This difference may be derived from the different conformations induced by the ribose structure.

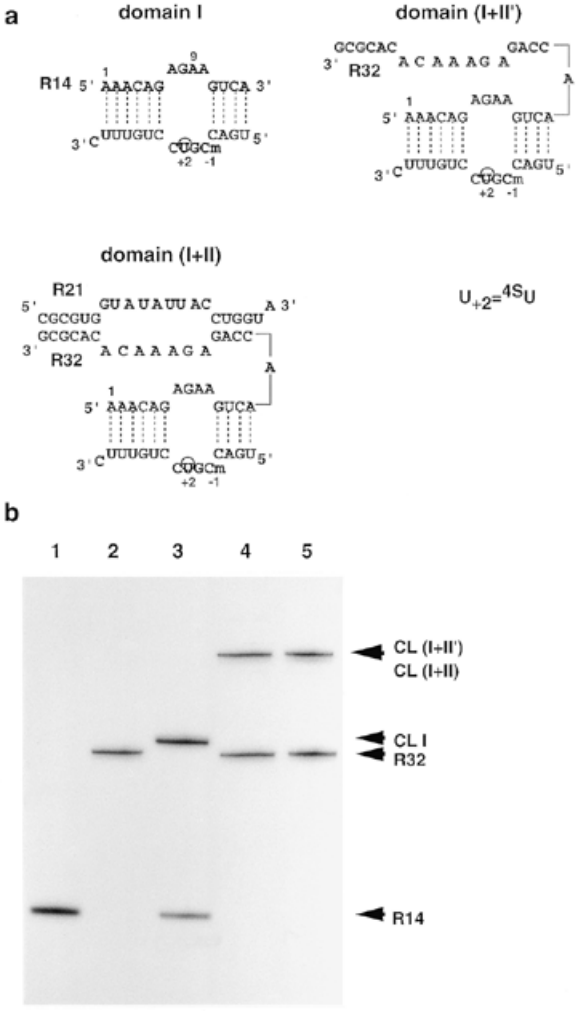

Figure 3. Photo crosslinking of 4-thiouridine. (**a**) Sequences of the three complexes used for photo crosslinking. ^{4S}U+2 in the substrate is circled. C-1 is substituted for 2′-*O*-methylcytidine in S-4S(me). Dotted and solid lines indicate base pairs and covalent bonds, respectively. (**b**) Denaturing polyacrylamide gel electrophoresis of the photo crosslinking reaction. Lane 1, ^{32}pR14; lane 2, ^{32}pR32; lane 3, photo crosslink of domain I [^{32}pR14+S-4S(me)]; lane 4, photo crosslink of domain (I+II′) [^{32}pR32+S-4S(me)]; lane 5, photo crosslink of domain (I+II) [^{32}pR32+R21+S-4S(me)]. CL I, CL (I+II′) and CL (I+II) indicate the crosslinked products of domain I, domain (I+II′) and domain (I+II), respectively.

CD measurements

The CD spectra of ^{4S}U and ^{2S}U have been measured for conformational analyses of tRNA, since these nucleosides indicate characteristic positive and negative peaks at 330 nm, respectively (55). Since the CD spectrum around 330 nm is derived from only the thiocarbonyl group, comparison of the CD spectra at 330 nm provides information about the conformational change of U+2 in domains I and (I+II). The CD spectra of domains I and (I+II) containing S-2S(me) or S-4S(me) in the substrate strand were measured at various temperatures. Both of these substrate strands had a 2′-*O*-methyl ribonucleoside (me) at the cleavage site, to prevent cleavage of the RNA during the CD measurement. Both complexes indicated a positive or negative peak around 330 nm, which was derived from ^{4S}U+2 or ^{2S}U+2 (Fig. 5a and b). When S-4S(me) containing ^{4S}U+2 was used as a substrate strand, domain (I+II) showed a peak with higher intensity than domain I at low temperature (Fig. 5a). This result suggests that the structure of ^{4S}U+2 was different between domains I and (I+II). On the other hand, when S-2S(me) was used as a substrate, there were few differences between the peak intensities from domains I and (I+II), even at low temperature (Fig. 5b). This result suggests that the environment around the 2-thiocarbonyl group of ^{2S}U+2 did not change between domain I alone and domain (I+II). Therefore, the environment near the 4-keto group of U+2 changes more than that around the 2-keto group of U+2 during domain docking, and this is consistent

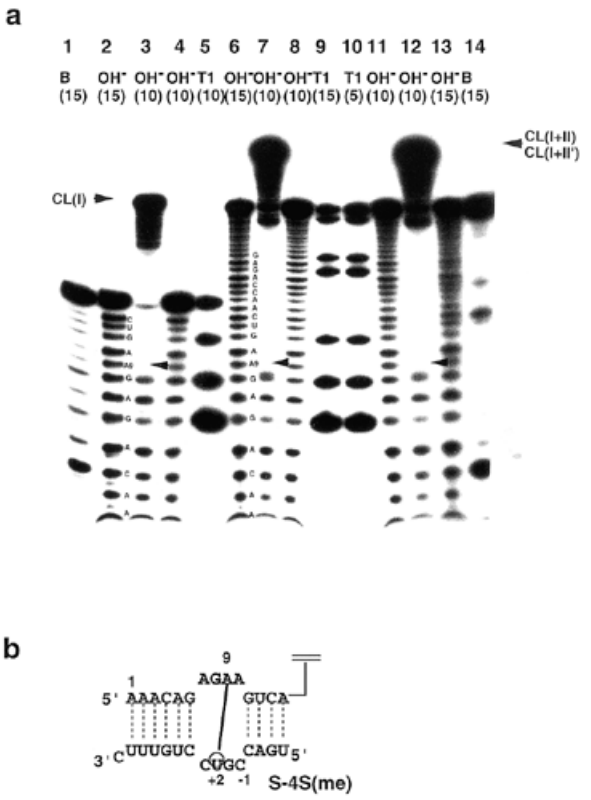

Figure 4. Identification of crosslinking residues in the complexes. (**a**) Analysis of crosslinking sites in R14 and R32. Lanes 1, 2, 4 and 5, partial alkaline hydrolysis and ribonucleases T1 and *B.cereus* digestion of ^{32}pR14 for markers; lane 3, partial alkaline hydrolysis of CL I [^{32}pR14-S-4S(me)]; lanes 6, 8, 9, 10, 11 and 14, partial alkaline hydrolysis and ribonucleases T1 and *B.cereus* digestion of ^{32}pR32 for markers; lanes 7 and 12, partial alkaline hydrolysis of CL (I+II′) [^{32}pR32-S-4S(me)] and CL (I+II) [^{32}pR32-S-4S(me)], respectively. Arrows indicate crosslinking sites in R14 and R32. Reaction times (min) are indicated in parentheses. (**b**) Secondary structure of ribozymes, showing the crosslink between A9 and ^{4S}U+2.

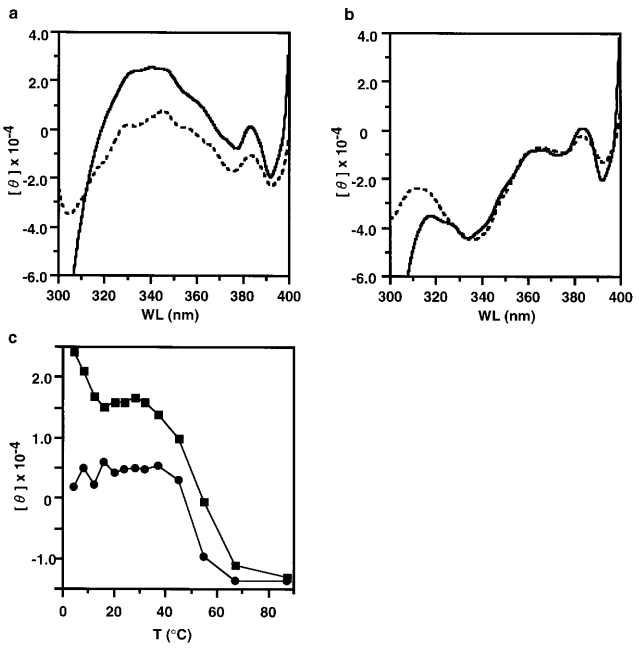

Figure 5. CD spectra of components of the hairpin ribozyme. CD spectra in the near UV region of domains I and (I+II) containing 4-thiouridine (**a**) or 2-thiouridine at 4°C (**b**). Domain I, dotted line; domain (I+II), solid line. (**c**) Plots of [θ] at 335 nm containing the ^{4S}U+2 versus various temperatures. Domain I, circles; domain (I+II), squares.

with the result from the cleavage reaction of the substrate with ^{4S}U. The peak intensities at 335 nm of domains I and (I+II) containing ^{4S}U+2 were plotted versus the temperature (Fig. 5c). The difference between the peak intensities from domains I and (I+II) became larger at a low temperature. The change at 50°C, found in both complexes, was derived from the destruction of the A-form structure, because the positive peak at 260 nm from the A-form structure also drastically changed at ~50°C. However, the peak intensity from domain (I+II) increased below 16°C, in contrast to that from domain I. It is thought that the difference is derived from the environmental change at ^{4S}U+2 caused by domain docking.

Watanabe and co-workers investigated the structures of 2- and 4-thiouridine in tRNA by comparing the reactivities of these bases with H_2O_2, which can promote desulfurization of 2- or 4-thiouridine (55,56), and the difference in the reactivities appeared around 330 nm in the CD spectra. Therefore, we investigated the reactivities of both ^{2S}U+2 and ^{4S}U+2 in domains I or (I+II) by CD measurements. As reported previously, 4-thiouridine reacted with H_2O_2 much faster than 2-thiouridine under the same conditions. Therefore, both domain I and domain (I+II) containing S-4S(me) were reacted with H_2O_2 under milder conditions than those for the domains containing S-2S(me). The reaction rate constants are listed in Table 2. ^{2S}U+2 in domain (I+II) reacted with H_2O_2 3-fold faster than that in domain I. On the other hand, the reactivity of ^{4S}U+2 in domain (I+II) decreased 2-fold faster than in domain I. When the two domains could interact with each other, such as in domain (I+II), the reaction of ^{4S}U+2 with H_2O_2 was prevented, whereas the reactivity of ^{2S}U+2 was enhanced. There was no difference in the reactivity of ^{4S}U+2 between both complexes in the absence of magnesium ions, which are important for domain docking. The reactivity of ^{4S}U+2 in both complexes was also the same at a higher temperature (32°C). These results suggest that the lower reactivity of ^{4S}U+2 in domain (I+II) was caused by domain docking and the conformational change of U+2. Based on the results from the previous NMR report and the present pyrimidine-substituted experiments, the conformation of U+2 in the substrate strand may change, as shown in Figure 6. In an inactive conformation, U+2 does not interact with any residues; however, in an active bent conformation, U+2 might change from the splayed structure to the helix.

Gait and co-workers presented a hairpin ribozyme model based on the results of the formation of an inter-domain disulfide bond (57). In this model, U+2 is located in the minor groove, the O4 of U+2 forms a hydrogen bond with the 2-amino group of G8 in the opposite strand, and the O2 of U+2 does not contact any nucleoside. However, the existence of the base pair has not been confirmed. On the other hand, the NMR result of domain I indicates that U+2 following the cleavage site does

Table 2. Reaction rates for 2- or 4-thiouridine in domains I and (I+II)

Complex	U+2	$[Mg^{2+}]$ (mM)	k (min^{-1})	$t_{1/2}$ (min)
Domain I	^{2S}U	12	1.5×10^{-3}	447
Domain (I+II)	^{2S}U	12	4.5×10^{-3}	129
Domain I	^{4S}U	0	3.0×10^{-3}	295
Domain (I+II)	^{4S}U	0	3.1×10^{-3}	237
Domain I	^{4S}U	12	1.5×10^{-2}	53
Domain (I+II)	^{4S}U	12	6.7×10^{-3}	98

Complexes containing ^{2S}U or ^{4S}U were reacted in the presence of 0.4 or 0.01% H_2O_2.

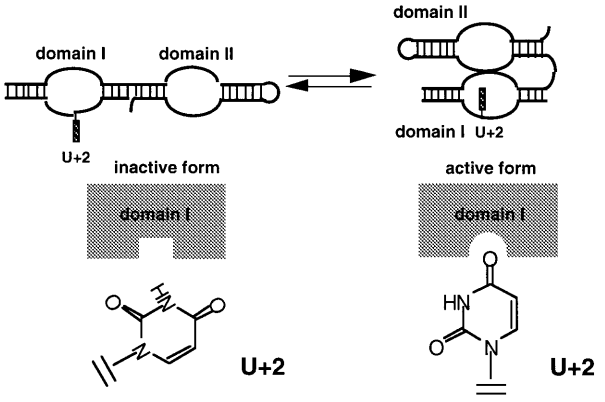

Figure 6. Schematic drawing of the conformational change of U+2 in domain docking.

not contact any base and is splayed apart. Furthermore, the NMR data suggest that U+2 adopts a millisecond conformational change (38). In our photo crosslinking experiment, there were few differences in either the crosslinked sites or the yields between domains I and (I+II). The reason for this is not clear. Due to the flexible conformation of U+2 in domain I alone, the equilibrium between the splayed structure and the stacked form might shift to the stacked structure during the UV-irradiation. Therefore, we think that the crosslinking reaction did not reflect the percentage of the stacked structure of U+2 exactly, but rather indicated the base stacking on U+2. Since A9 stacks with U+2 in the model, the present result that ^{4S}U+2 crosslinked with A9 agrees with the structure in the model. The pyrimidine substitution experiments performed here suggest that the O4 of U+2 is involved in the hydrogen bond, but the O2 is not. Thus, the O4 of U+2 may be recognized by the 2-amino group of G8 by domain docking, as shown in the predicted model. Together with the results from NMR studies, the substitution experiments performed here suggest that U+2 in loop A is in a splayed out structure at the ground state and moves to the minor groove during the cleavage reaction. The O4 of U+2 may be involved in the transition state.

SUPPLEMENTARY MATERIAL

See Supplementary Material available in NAR Online.

ACKNOWLEDGEMENTS

We thank Dr M. J. Gait and Dr E. Westhof for the coordinates of the hairpin ribozyme model, Dr S. Ichikawa (Hokkaido University) for suggestions regarding the synthesis of 2-thiouridine, Dr K. Watanabe for CD measurement and Y. Misawa (Hokkaido University) for technical assistance. This work was supported by a Grant-in-Aid from the Ministry of Education, Science, Sports and Culture of Japan.

REFERENCES

1. Buzayan,J.M., Gerlach,W.L. and Bruening,G. (1986) *Nature*, **323**, 349–353.
2. Symons,R.H. (1992) *Annu. Rev. Biochem.*, **61**, 641–671.
3. Hampel,A. and Triz,R. (1989) *Biochemistry*, **28**, 4929–4933.
4. Hampel,A., Triz,R., Hicks,M. and Cruz,P. (1990) *Nucleic Acids Res.*, **18**, 299–304.
5. Van Tol,H., Buzayan,J.M., Feldstein,P.A., Eckstein,F. and Bruening,G. (1990) *Nucleic Acids Res.*, **18**, 1971–1975.
6. Hampel,A. (1998) *Progress Nucleic Acid Res. Mol. Biol.*, **58**, 1–39.
7. Dahm,S.C. and Uhlenbeck,O.C. (1991) *Biochemistry*, **30**, 9464–9469.
8. Chowrira,B.M., Berzal-Herranz,A. and Burke,J.M. (1993) *Biochemistry*, **20**, 1088–1095.
9. Walter,N.G. and Burke,J.M. (1998) *Curr. Opin. Chem. Biol.*, **2**, 24–30.
10. Buzayan,J.M., Feldstein,P.A., Bruening,G. and Eckstein,F. (1988) *Biochem. Biophys. Res. Commun.*, **156**, 340–347.
11. Koizumi,M. and Ohtsuka,E. (1991) *Biochemistry*, **30**, 5145–5150.
12. Hampel,A. and Cowan,J.A. (1997) *Chem. Biol.*, **4**, 513–517.
13. Nesbitt,S., Hegg,L.A. and Fedor,M.J. (1997) *Chem. Biol.*, **4**, 619–630.
14. Young,K.J., Gill,F. and Grasby,J.A. (1997) *Nucleic Acids Res.*, **25**, 3760–3766.
15. Earnshaw,D.J. and Gait,M.J. (1998) *Nucleic Acids Res.*, **26**, 5551–5561.
16. Anderson,P., Monforte,J., Tritz,R., Nesbitt,S., Hearst,J. and Hampel,A. (1994) *Nucleic Acids Res.*, **22**, 1096–1100.
17. Chowrira,B.M., Berzal-Herranz,A. and Burke,J.M. (1991) *Nature*, **354**, 320–322.
18. Berzal-Herranz,A., Joseph,S. and Burke,J.M. (1992) *Genes Dev.*, **6**, 129–134.
19. Berzal-Herranz,A., Joseph,S., Chowrira,B.M., Butcher,S.E. and Burke,J.M. (1993) *EMBO J.*, **12**, 2567–2574.
20. Feldstein,P.A. and Bruening,G. (1993) *Nucleic Acids Res.*, **21**, 1991–1998.
21. Komatsu,Y., Koizumi,M., Nakamura,H. and Ohtsuka,E. (1994) *J. Am. Chem. Soc.*, **116**, 3692–3696.
22. Komatsu,Y., Kanzaki,I., Koizumi,M. and Ohtsuka,E. (1995) *J. Mol. Biol.*, **252**, 296–304.
23. Komatsu,Y., Kanzaki,I. and Ohtsuka,E. (1996) *Biochemistry*, **35**, 9815–9820.
24. Murchie,A.I.H., Thomson,J.B., Walter,F. and Lilley,D.M.J. (1998) *Mol. Cell*, **1**, 873–881.
25. Walter,F., Murchie,A.I.H. and Lilley,D.M.J. (1998) *Biochemistry*, **37**, 17629–17636.
26. Esteban,J.A., Walter,N.G., Kotzorek,G., Heckman,J.E. and Burke,J.M. (1998) *Proc. Natl Acad. Sci. USA*, **95**, 6091–6096.
27. Hegg,L.A. and Fedor,M.J. (1995) *Biochemistry*, **34**, 15813–15828.
28. Esteban,J.A., Banerjee,A.R. and Burke,J.M. (1997) *J. Biol. Chem.*, **272**, 13629–13639.
29. Butcher,S.E. and Burke,J.M. (1994) *J. Mol. Biol.*, **244**, 52–63.
30. Butcher,S.E. and Burke,J.M. (1994) *Biochemistry*, **33**, 992–999.
31. dos Santos,D.V., Fourrey,J.L. and Favre,A. (1993) *Biochem. Biophys. Res. Commun.*, **190**, 377–385.
32. dos Santos,D.V., Vianna,A.-L., Fourrey,J.-L. and Favre,A. (1993) *Nucleic Acids Res.*, **21**, 201–207.
33. Grasby,J.A., Mersmann,K., Singh,M. and Gait,M.J. (1995) *Biochemistry*, **34**, 4068–4076.

34. Chowrira,B.M., Berzal-Herranz,A., Keller,C.F. and Burke,J.M. (1993) *J. Biol. Chem.*, **268**, 19458–19462.
35. Schmidt,S., Beigelman,L., Karpeisky,A., Usman,N., Sorensen,U.S. and Gait,M.J. (1996) *Nucleic Acids Res.*, **24**, 573–581.
36. Butcher,S.B., Allain,F.H.-T. and Feigon,J. (1999) *Nature Struct. Biol.*, **6**, 212–216.
37. Young,K.J., Vyle,J.S., Pickering,T.J., Cohen,M.A., Holmes,S.C., Merkel,O. and Grasby,J.A. (1999) *J. Mol. Biol.*, **288**, 853–866.
38. Cai,Z.P. and Tinoco,I. (1996) *Biochemistry*, **35**, 6026–6036.
39. Shippy,R., Siwkowski,A. and Hampel,A. (1998) *Biochemistry*, **37**, 564–570.
40. Miah,A., Reese,C.B. and Song,Q. (1997) *Nucl. Nucl.*, **16**, 53–65.
41. Shah,K., Wu,H. and Rana,T.M. (1994) *Bioconjugate Chem.*, **5**, 508–512.
42. Allerson,C.R., Chen,S.L. and Verdine,G.L. (1997) *J. Am. Chem. Soc.*, **119**, 7423–7433.
43. Kumar,R.K. and Davis,D.R. (1997) *Nucleic Acids Res.*, **25**, 1272–1280.
44. Kido,K., Inoue,H. and Ohtsuka,E. (1992) *Nucleic Acids Res.*, **20**, 1339–1344.
45. Grasby,J.A., Butler,P.J.G. and Gait,M.J. (1993) *Nucleic Acids Res.*, **21**, 4444–4450.
46. Adams,C.J., Murray,J.B., Arnold,J.R.P. and Stockley,P.G. (1994) *Tetrahedron Lett.*, **35**, 765–768.
47. Murray,J.B., Adams,C.J., Arnold,J.R.P. and Stockley,P.G. (1995) *Biochem. J.*, **311**, 487–494.
48. Hakimelahi,G.H., Proba,Z.A. and Ogilvie,K.K. (1982) *Can. J. Chem.*, **60**, 1106–1113.
49. Scaringe,S.A., Francklyn,C. and Usman,N. (1990) *Nucleic Acids Res.*, **18**, 5433–5441.
50. Igloi,G.L. (1988) *Biochemistry*, **27**, 3842–3849.
51. Komatsu,Y., Shirai,M., Yamashita,S. and Ohtsuka,E. (1997) *Bioorg. Med. Chem.*, **5**, 1063–1069.
52. Brennan,R.G., Prive,G.G., Blonski,W.J.P., Hruska,F.E. and Sundaralingam,M. (1983) *J. Am. Chem. Soc.*, **105**, 7737–7742.
53. Brennan,R.G., Pyzalska,D., Blonski,W.J.P., Hruska,F.E. and Sundaralingam,M. (1986) *Biochemistry*, **25**, 1181–1185.
54. Walter,N.G., Hampel,K.J., Brown,K.M. and Burke,J.M. (1998) *EMBO J.*, **17**, 2378–2391.
55. Watanabe,K. (1980) *Biochemistry*, **19**, 5542–5549.
56. Watanabe,K., Hayashi,N., Oyama,A., Nishikawa,K., Ueda,T. and Miura,K. (1993) *Nucleic Acids Res.*, **22**, 79–87.
57. Earnshaw,D.J., Masquida,B., Muller,S., Sigurdsson,S.T., Eckstein,F., Westhof,E. and Gait,M.J. (1997) *J. Mol. Biol.*, **274**, 197–212.